Table 2. Relationships in the after-effects of real-tDCS on MEP amplitude and IHI.

Measurements		Electrode montage					
		Anodal		Cathodal		Bilateral	
MEP	IHI	*r* value	*p* value	*r* value	*p* value	*r* value	*p* value
Left M1	Left to Right M1	−0.21	0.52	0.35	0.27	0.16	0.62
Left M1	Right to Left M1	−0.01	0.98	−0.30	0.35	−0.28	0.39
Right M1	Left to Right M1	−0.36	0.25	0.05	0.89	−0.27	0.39
Right M1	Right to Left M1	0.21	0.52	0.03	0.92	−0.32	0.31

Values were obtained by Pearson correlation analysis.

doi:10.1371/journal.pone.0114244.t002

relationships between the modulations of MEP amplitude and IHI. If IHI is mainly derived from the collateral discharges of corticospinal neurons and the tDCS-induced modulation in IHI resulted from the changes in collateral discharges, the modulations in MEP amplitude and IHI could have been correlated. Therefore, the modulation of transcallosal pathways could be partly independent of the changes in corticospinal descending pathways. Transcallosal inhibition is assumed to be derived from the discharge of callosal neurons that are distinct from corticospinal neurons [24, 28, 29]. Accordingly, tDCS might have similarly influenced both corticospinal and callosal neurons in the same M1. In some previous studies, IHI has been evaluated by matching the size of CS-induced MEPs in order to normalize the CS effect [24, 30, 31]. However, the adjusted CS intensity may not be sensitive enough to detect the excitability change in callosal neurons when both corticospinal and callosal neurons are modulated in parallel [24, 31, 32]. In the present study, we used the same CS intensity across before and after the tDCS sessions according to the RMT. Therefore, the modulation of IHI could be observed by detecting parallel modulation in the excitabilities of corticospinal and callosal neurons.

Our findings of the modulation of transcallosal inhibition are partly inconsistent with a previous study that used iSP [25], although the corticospinal excitability was modulated in a similar way. The previous study did not observe changes in iSP from the modulated M1 underneath the tDCS electrode [25]. One possible explanation for this discrepancy may be the differences in the tDCS parameters. The present experiments used a higher intensity (1.5 mA) and a longer duration (15 min) of tDCS compared to the previous study (1.0 mA intensity, 10 min duration). The tDCS after-effects have been shown to increase up to a certain extent of intensity and duration [12, 33, 34]. Furthermore, because the threshold for eliciting transcallosal inhibition is known to be higher than the RMT for MEPs [29, 35–37], callosal neurons might require a relatively high intensity and long duration of tDCS to be modulated. Another possibility is the different neural populations mediating transcallosal inhibition because partly different sets of callosal neurons and target neurons receiving callosal volleys have been assumed to mediate short-interval IHI and iSP [26]. In addition, iSP appears as the inhibition of static voluntary activity, although IHI is the inhibition of

synchronized corticospinal discharges that TMS artificially evokes [29]. Accordingly, such physiological differences might relate to the different susceptibilities to tDCS. Indeed, previous study using rTMS demonstrated the modulation of IHI without robust changes of iSP [27].

We also observed a reduction of IHI from the unchanged M1 after unilateral cathodal tDCS, although unilateral anodal tDCS did not modulate IHI from the unchanged M1. These findings suggested that unilateral tDCS affected interneuronal circuits that presynaptically regulate callosal transmission and/or relay them to the corticospinal neurons [25]. Indeed, tDCS-induced plastic modulation has been shown in some intracortical interneurons that mediate gamma-aminobutyric acid activity [38–40]. One potential reason that unilateral anodal tDCS failed to modulate IHI in this direction might be due to the asymmetry in transcallosal inhibition. Generally, transcallosal inhibition is greater from the left M1 to the right M1 than from the right M1 to the left M1 in right-handers [41, 42], which was also confirmed in our study. Furthermore, previous study reported asymmetric effects of tDCS [4]; tDCS applied over the left dominant hemisphere was more effective than that over the right non-dominant hemisphere. In our study, anodal and cathodal stimuli were given to the different hemispheres. Hence, the lack of modulation of IHI toward the facilitated right-side M1 might be also attributed to the decreased efficiency of tDCS that is applied over the non-dominant hemisphere.

The effect of interventional brain stimulation on transcallosal inhibition has been tested by several stimulation protocols such as low-frequency rTMS [27, 43], theta burst stimulation [44, 45], paired associative stimulation [46], tDCS [5, 25], and quadripulse TMS [47]. Even though their protocols were able to elicit bidirectional modulation on the corticospinal excitability, the modulation of transcallosal inhibition was not always observed [44, 45]. Presumably, the neural elements involving with transcallosal inhibition might have different susceptibilities according to the type of brain stimulation protocol. Although our results show that bilateral tDCS was able to elicit the bidirectional modulation in transcallosal inhibition between left M1 and right M1 in addition to the left and right corticospinal excitabilities, it is worth noting that the extent of MEP modulation by bilateral tDCS was not different compared to that by unilateral tDCS. This finding was also reported in recent studies [16, 17]. Additionally, in line with previous studies [16, 25, 48], neither the polarity of unilateral tDCS affected the corticospinal excitability in the contralateral unstimulated motor cortex even though transcallosal inhibition toward that motor cortex showed short-lasting after-effects (Figure 1). These findings suggest that transcallosal inhibition modulated by tDCS might have minor static effects on the corticospinal excitability in the contralateral motor cortex. Nevertheless, previous studies demonstrated that bilateral tDCS was more effective for improving hand motor performance compared to unilateral anodal tDCS over the target motor cortex [3, 10], and that unilateral cathodal tDCS over a motor cortex results in substantial improvement of ipsilateral hand motor function in healthy [2, 4] and stroke individuals [7, 9, 11, 49]. These facts could provide us rationale to suppose

that suppressed transcallosal inhibition contributes to the contralateral cortical motor activity. Indeed, Williams et al. [5] demonstrated a functional relationship between the suppression of transcallosal inhibition and improvements in motor performance using bilateral tDCS. Conceivably, it might be that a functional role of the decreased transcallosal inhibition can be observed in a time-specific motor event like movement initiation. Transcallosal inhibition is gradually decreased according to the time course of movement initiation [50, 51]. Therefore, a sustained reduction of transcallosal inhibition could contribute to such a situation of motor performance rather than a static enhancement of corticospinal excitability. To support this notion, recent studies using functional magnetic resonance imaging demonstrated that motor task-related M1 activation was greater in bilateral tDCS compared to unilateral anodal tDCS, and that the M1 activation changes in laterality were correlated with microstructural status of transcallosal motor fibers [18] although resting-state interhemispheric functional connectivity between the left M1 and the right M1 did not show after-effects regardless of unilateral anodal or bilateral tDCS [20]. Therefore, it seems conceivable that modulated transcallosal pathways contribute to the motor performances without marked changes in the corticospinal excitability at rest.

From the methodological point of view, we need to consider tDCS parameters as limitations of our study. First, strong intensity and long duration of direct current stimulation has a risk of over stimulating that causes reversing facilitatory effect of cathodal tDCS on the corticospinal excitability. A recent study demonstrated that cathodal tDCS with 2 mA of intensity and 20 min of duration facilitated the corticospinal excitability [52]. Because tDCS with a high intensity (2 mA) and a short duration (5 min) retained the general polarity-specific after-effects [16], the combination of intensity and duration might be a specific factor for the tDCS after-effects. Second, small number of participants should be considered as another limitation. Though we found significant tDCS after-effects on MEP amplitude and IHI, some insignificant results may be due to small sample size. We should make a point that the participants were not completely identical across real-tDCS and sham-tDCS sessions. Finally, our study cannot completely rule out spinal effects [53, 54]. Though IHI was demonstrated to be mediated by cortical circuits through transcallosal pathways [55, 56], potential contribution of subcortical circuits to IHI need to be considered [57].

As a therapeutic tool, tDCS has been frequently applied in patients with hemiparetic stroke [58]. Thus, our findings that tDCS modulated transcallosal inhibition with polarity-specific manner could provide a useful perspective on the understanding of the tDCS therapeutic effect on the recovery of motor function after stroke. In terms of interhemispheric neural modulations, the application of cathodal tDCS to contralesional hemisphere appears to be reliable as demonstrated by some clinical studies [7, 8, 10, 11, 49]. However, we may also need to take into account the tDCS effect on the uncrossed ipsilateral motor pathway [59, 60]. A recent study demonstrated that cathodal tDCS over a motor cortex affected presumed uncrossed cortico-propriospinal pathway [60]. As the severely impaired motor function is potentially compensated by ipsilateral cortical activity

[61], it is important to note the potential risk that cathodal stimulation over ipsilesional hemisphere deteriorates motor function [62].

In conclusion, the present study demonstrated that tDCS produced polarity-specific after-effects on transcallosal inhibition between motor cortices. Comprehensively, IHI was increased from the M1 at which the corticospinal excitability was increased and decreased from the M1 at which the corticospinal excitability was decreased, suggest that tDCS is capable of modulating neuronal activities that are involved with sending and receiving callosal discharges.

Acknowledgments

We would like to thank Dr. Y. Nakajima for his support. We also thank Mr. T. Hoshiba for assistance of data collection.

Author Contributions

Conceived and designed the experiments: TT TE TO. Performed the experiments: TT TE TK. Analyzed the data: TT. Contributed reagents/materials/analysis tools: TT TE TO. Wrote the paper: TT TO.

References

1. **Boggio PS, Castro LO, Savagim EA, Braite R, Cruz VC, et al.** (2006) Enhancement of non-dominant hand motor function by anodal transcranial direct current stimulation. Neurosci Lett 404: 232–236.
2. **Vines BW, Nair DG, Schlaug G** (2006) Contralateral and ipsilateral motor affects after transcranial direct current stimulation. NeuroReport 17: 671–674.
3. **Vines BW, Cerruti C, Schlaug G** (2008) Dual-hemisphere tDCS facilitates greater improvements for healthy subjects' non-dominant hand compared to uni-hemisphere stimulation. BMC Neurosci 9: 103. doi: 10.1186/1471-2202-9-103
4. **Vines BW, Nair D, Schlaug G** (2008) Modulating activity in the motor cortex affects performance for the two hands differently depending upon which hemisphere is stimulated. Eur J Neurosci 28: 1667–1673.
5. **Williams JA, Pascual-Leone A, Fregni F** (2010) Interhemispheric modulation induced by cortical stimulation and motor training. Phys Ther 90: 398–410.
6. **Waters-Metenier S, Husain M, Wiestler T, Diedrichsen J** (2014) Bihemispheric transcranial direct current stimulation enhances effector-independent representations of motor synergy and sequence learning. J Neurosci 34: 1037–1050.
7. **Fregni F, Boggio PS, Mansur CG, Wagner T, Ferreira MJ, et al.** (2005) Transcranial direct current stimulation of the unaffected hemisphere in stroke patients. NeuroReport 16: 1551–1555.
8. **Hummel F, Celnik P, Giraux P, Floel A, Wu WH, et al.** (2005) Effects of non-invasive cortical stimulation on skilled motor function in chronic stroke. Brain, 128: 490–499.
9. **Boggio PS, Nunes A, Rigonatti SP, Nitsche MA, Pascual-Leone A, et al.** (2007) Repeated sessions of noninvasive brain DC stimulation is associated with motor function improvement in stroke patients. Restor Neurol Neurosci 25: 123–129.
10. **Mahmoudi H, Borhani Haghighi A, Petramfar P, Jahanshahi S, et al.** (2011) Transcranial direct current stimulation: electrode montage in stroke. Disabil Rehabil 33: 1383–1388.
11. **Zimerman M, Heise KF, Hoppe J, Cohen LG, Gerloff C, et al.** (2012) Modulation of training by single-session transcranial direct current stimulation to the intact motor cortex enhances motor skill acquisition of the paretic hand. Stroke 43: 2185–2191.

12. **Nitsche MA, Paulus W** (2000) Excitability changes induced in the human motor cortex by weak transcranial direct current stimulation. J Physiol (Lond) 527: 633–639.

13. **Hummel FC, Cohen LG** (2006) Non-invasive brain stimulation: a new strategy to improve neurorehabilitation after stroke? Lancet Neurol 5: 708–712.

14. **Kobayashi M, Théoret H, Pascual-Leone A** (2009) Suppression of ipsilateral motor cortex facilitates motor skill learning. Eur J Neurosci 29: 833–836.

15. **Kang EK, Paik NJ** (2011) Effect of a tDCS electrode montage on implicit motor sequence learning in healthy subjects. Exp Transl Stroke Med 3: 4.

16. **Mordillo-Mateos L, Turpin-Fenoll L, Millán-Pascual J, Núñez-Pérez N, Panyavin I, et al.** (2012) Effects of simultaneous bilateral tDCS of the human motor cortex. Brain Stimul 5: 214–222.

17. **Kidgell DJ, Goodwill AM, Frazer AK, Daly RM** (2013) Induction of cortical plasticity and improved motor performance following unilateral and bilateral transcranial direct current stimulation of the primary motor cortex. BMC Neurosci 14: 64.

18. **Lindenberg R, Nachtigall L, Meinzer M, Sieg MM, Flöel A** (2013) Differential effects of dual and unihemispheric motor cortex stimulation in older adults. J Neurosci, 33: 9176–9183.

19. **O'Shea J, Boudrias M-H, Staggg CJ, Bachtiar V, Kischka U, et al.** (2013) Predicting behavioral response to TDCS chronic motor stroke. NeuroImage 85: 924–933.

20. **Sehm B, Kipping J, Schäfer A, Villringer A, Ragert P** (2013) A comparison between uni- and bilateral tDCS effects on functional connectivity of the human motor cortex. Front Hum Neurosci, 7, 183. doi: 10.3389/fnhum.2013.00183

21. **Daskalakis ZJ, Christensen BK, Fitzgerald PB, Roshan L, Chen R** (2002) The mechanisms of interhemispheric inhibition in the human motor cortex. J Physiol (Lond) 543: 317–326.

22. **Kukaswadia S, Wagle-Shukla A, Morgante F, Gunraj C, Chen R** (2005) Interactions between long latency afferent inhibitions in the human motor cortex. J Physiol (Lond) 563: 915–924.

23. **Avanzino L, Teo JTH, Rothwell JC** (2007) Intracortical circuits modulate transcallosal inhibition in humans. J Physiol (Lond) 583: 99–114.

24. **Lee H, Gunraj C, Chen R** (2007) The effects of inhibitory and facilitatory intracortical circuits on interhemispheric inhibition in the human motor cortex. J Physiol (Lond) 580: 1021–1032.

25. **Lang N, Nitsche MA, Paulus W, Rothwell JC, Lemon RN** (2004) Effects of transcranial direct current stimulation over the human motor cortex on corticospinal and transcallosal excitability. Exp Brain Res 156: 439–443.

26. **Chen R, Yung D, Li JY** (2003) Organization of ipsilateral excitatory and inhibitory pathways in the human motor cortex. J Neurophysiol, 89: 1256–1264.

27. **Gilio F, Rizzo V, Siebner HR, Rothwell JC** (2003) Effects on the right motor hand-area excitability produced by low-frequency rTMS over human contralateral homologous cortex. J Physiol (Lond) 551: 563–573.

28. **Catsman-Berrevoets CE, Lemon RN, Verburgh CA, Bentivoglio M, Kuypers HG** (1980) Absence of callosal collaterals derived from rat corticospinal neurons. A study using fluorescent retrograde tracing and electrophysiological techniques. Exp Brain Res 39: 433–440.

29. **Ferbert A, Priori A, Rothwell JC, Day BL, Colebatch JG, et al.** (1992) Interhemispheric inhibition of the human motor cortex. J Physiol (Lond) 453: 525–546.

30. **Perez MA, Cohen LG** (2008) Mechanisms underlying functional changes in the primary motor cortex ipsilateral to an active hand. J Neurosci 28: 5631–5640.

31. **Nelson AJ, Hoque T, Gunraj C, Ni Z, Chen R** (2009) Bi-directional interhemispheric inhibition during unimanual sustained contractions. BMC Neurosci 10, 31. doi: 10.1186/1471-2202-10-31

32. **Hinder MR, Schmidt MW, Garry MI, Summers JJ** (2010) Unilateral contractions modulate interhemispheric inhibition most strongly and most adaptively in the homologous muscle of the contralateral limb. Exp Brain Res 205: 423–433.

33. **Nitsche MA, Paulus W** (2001) Sustained excitability elevations induced by transcranial DC motor cortex stimulation in humans. Neurol 57: 1899–1901.

34. **Nitsche MA, Nische MS, Klein CC, Tergau F, Rothwell JC, et al.** (2003) Level of action of cathodal DC polarisation induced inhibition of the human motor cortex. Clin Neurophysiol 114: 600–604.

35. **Trompetto C, Buccolieri A, Marchese R, Marinelli L, Michelozzi G, et al.** (2003) Impairment of transcallosal inhibition in patients with corticobasal degeneration. Clin Neurophysiol 114: 2181–2187.

36. **Tsutsumi R, Shirota Y, Ohminami S, Terao Y, Ugawa Y, et al.** (2012) Conditioning intensity-dependent interaction between short-latency interhemispheric inhibition and short-latency afferent inhibition. J Neurophysiol 108: 1130–1137.

37. **Tazoe T, Sasada S, Sakamoto M, Komiyama T** (2013) Modulation of interhemispheric interactions across symmetric and asymmetric bimanual force regulations. Eur J Neurosci, 37: 96–104.

38. **Nitsche MA, Seeber A, Frommann K, Klein CC, Rochford C, et al.** (2005) Modulating parameters of excitability during and after transcranial direct current stimulation of the human motor cortex. J Physiol (Lond) 568: 291–303.

39. **Scelzo E, Giannicola G, Rosa M, Ciocca M, Ardolino G, et al.** (2011) Increased short latency afferent inhibition after anodal transcranial direct current stimulation. Neurosci Lett 498: 167–170.

40. **Tremblay S., Beaulé V, Lepage JF, Théoret H** (2013) Anodal transcranial direct current stimulation modulates GABAB-related intracortical inhibition in the M1 of healthy individuals. NeuroReport 24, 46–50.

41. **Netz J, Ziemann U, Hömberg V** (1995) Hemispheric asymmetry of transcallosal inhibition in man. Exp Brain Res 104: 527–533.

42. **Bäumer T, Dammann E, Bock F, Klöppel S, Siebner HR, et al.** (2007) Laterality of interhemispheric inhibition depends on handedness. Exp Brain Res 180: 195–203.

43. **Pal PK, Hanajima R, Gunraj CA, Li JY, Wagle-Shukla A, et al.** (2005) Effect of low-frequency repetitive transcranial magnetic stimulation on interhemispheric inhibition. J Neurophysiol 94: 1668–1675.

44. **Di Lazzaro V, Pilato F, Dileone M, Profice P, Oliviero A, et al.** (2008) The physiological basis of the effects of intermittent theta burst stimulation of the human motor cortex. J Physiol (Lond) 586: 3871–3879.

45. **Suppa A, Ortu E, Zafar N, Deriu F, Paulus W, et al.** (2008) Theta burst stimulation induces after-effects on contralateral primary motor cortex excitability in humans. J Physiol (Lond) 586: 4489–4500.

46. **Shin H-W, Sohn YH** (2011) Interhemispheric transfer of paired associative stimulation-induced plasticity in the human motor cortex. NeurReport 22: 166–170.

47. **Tsutsumi R, Hanajima R, Terao Y, Shirota Y, Ohminami S, et al.** (2013) Effects of the motor cortical quadripulse transcranial magnetic stimulation (QPS) on the contralateral motor cortex and interhemispheric interactions. J Neurophysiol 111: 26–35.

48. **Di Lazzaro V, Manganelli F, Dileone M, Notturno F, Esposito M, et al.** (2012) The effects of prolonged cathodal direct current stimulation on the excitability and inhibitory circuits of the ipsilateral and contralateral motor cortex. J Neural Transm 119: 1499–1506.

49. **Kim DY, Lim JY, Kang EK, You DS, Oh MK, et al.** (2010) Effect of transcranial direct current stimulation on motor recovery in patients with subacute stroke. Am J Phys Med Rehabil 89: 879–886.

50. **Duque J, Murase N, Celnik P, Hummel F, Harris-Love M, et al.** (2007) Intermanual differences in movement-related interhemispheric inhibition. J Cogn Neurosci 19: 204–213.

51. **Tazoe T, Perez MA** (2013) Speed-dependent contribution of callosal pathways to ipsilateral movements. J Neurosci 33: 16178–16188.

52. **Batsikadze G, Moliadze V, Paulus W, Kuo MF, Nitsche MA** (2013) Partially non-linear stimulation intensity-dependent effects of direct current stimulation on motor cortex excitability in humans. J Physiol (Lond) 591: 1987–2000.

53. **Roche N, Lackmy A, Achache V, Bussel B, Katz R** (2009) Impact of transcranial direct current stimulation on spinal network excitability in humans. J Physiol (Lond) 587: 5653–5664.

54. **Roche N, Lackmy A, Achache V, Bussel B, Katz R** (2012) Effect of anodal tDCS on lumber propirospinal system in healthy subjects. Clin Neurophysiol 123: 1027–1034.

55. **Di Lazzaro V, Oliviero A, Profice P, Insola A, Mazzone P, et al.** (1999) Direct demonstration of interhemispheric inhibition of the human motor cortex produced transcranial magnetic stimulation. Exp Brain Res 124: 520–524.

56. **Li J-Y, Lai P-H, Chen R** (2013) Transcallosal inhibition in patients with callosal infarction. J Neurophysiol 109: 659–665.

57. **Gerloff C, Cohen LG, Floeter MK, Chen R, Corwell B, et al.** (1999) Inhibitory influence of the ipsilateral motor cortex on responses to stimulation of the human cortex and pyramidal tract. J Physiol (Lond) 510: 249–259.

58. **Nowak DA, Grefkes C, Ameli M, Fink GR** (2009) Interhemispheric competition after stroke: brain stimulation to enhance recovery of function of the affected hand. Neurorehabil Neural Repair 23: 641–656.

59. **Tazoe T, Perez MA** (2014) *Selective activation of ipsilateral motor pathways in intact humans.* J Neurosci 34: 13924–13934.

60. **Bradnam LV, Stinear CM, Byblow WD** (2011) Cathodal transcranial direct current stimulation suppresses ipsilateral projections to presumed propriospinal neurons of the proximal upper limb. J Neurophysiol 105: 2582–2589.

61. **Rehme AK, Fink GR, von Cramon DY, Grefkes C** (2011) The role of the contralesional motor cortex for motor recovery in the early days after stroke assessed with longitudinal FMRI. Cereb Cortex 21: 756–768.

62. **Bradnam LV, Stinear CM, Barber PA, Byblow WD** (2012) Contralesional hemisphere control of the proximal paretic upper limb following stroke. Cereb Cortex 22: 2662–2671.

Neuroscience Letters 584 (2015) 337–341

Contents lists available at ScienceDirect

Neuroscience Letters

journal homepage: www.elsevier.com/locate/neulet

Velocity-dependent suppression of the soleus H-reflex during robot-assisted passive stepping

Yohei Masugi[a,*], Taku Kitamura[b,c], Kiyotaka Kamibayashi[d], Tetsuya Ogawa[e], Toru Ogata[c], Noritaka Kawashima[c], Kimitaka Nakazawa[a]

[a] Department of Life Sciences, Graduate School of Arts and Sciences, The University of Tokyo, 3-8-1 Komaba, Meguro-ku, Tokyo 153-8902, Japan
[b] Division of Functional Control Systems, Graduate School of Engineering and Science, Shibaura Institute of Technology, 307, Fukasaku, Minuma-ku, Saitama-shi, Saitama 337-8570, Japan
[c] Department of Motor Dysfunction, Research Institute of National Rehabilitation Center for the Disabled, 4-1 Namiki, Tokorozawa-shi, Saitama 359-8555, Japan
[d] Faculty of Health and Sports Science, Doshisha University, 1-3 Tatara Miyakodani, Kyotanabe-shi, Kyoto 610-0394, Japan
[e] Faculty of Sport Sciences, Graduate School of Sport Sciences, Waseda University, 2-579-15, Mikajima, Tokorozawa-shi, Saitama 359-1192, Japan

HIGHLIGHTS

- The effect of passive stepping velocity on the soleus H-reflex was studied.
- The H-reflexes were smaller during passive stepping than standing.
- The H-reflexes significantly decreased at faster stepping velocities.

ARTICLE INFO

Article history:
Received 7 June 2014
Received in revised form
17 September 2014
Accepted 26 October 2014
Available online 3 November 2014

Keywords:
Hoffmann reflex
Afferent input
Locomotion
Velocity
Passive stepping

ABSTRACT

The amplitude of the Hoffmann (H)-reflex in the soleus (Sol) muscle is known to be suppressed during passive stepping compared with during passive standing. The reduction of the H-reflex is not due to load-related afferent inputs, but rather to movement-related afferent inputs from the lower limbs. To elucidate the underlying neural mechanisms of this inhibition, we investigated the effects of the stepping velocity on the Sol H-reflex during robot-assisted passive stepping in 11 healthy subjects. The Sol H-reflexes were recorded during passive standing and stepping at five stepping velocities (stride frequencies: 14, 21, 28, 35, and 42 min^{-1}) in the air. The Sol H-reflexes were significantly inhibited during passive stepping as compared with during passive standing, and reduced in size as the stepping velocity increased. These results indicate that the extent of H-reflex suppression increases with increasing movement-related afferent inputs from the lower limbs during passive stepping. The velocity dependence suggests that the Ia afferent inputs from lower-limb muscles around the hip and knee joints are most probably related to this inhibition.

1. Introduction

It is well known that the amplitude of the soleus (Sol) Hoffman (H)-reflex is strongly modulated in a task-dependent manner [2,3]. For example, the Sol H-reflex is significantly reduced during walking compared with during standing [2], and is further reduced during running compared with during walking [3]. Although presynaptic inhibition of Ia terminals is conceived to be a key mechanism in task-dependent H-reflex modulation [2,3], it is not yet fully understood to what extent, and how afferent inputs during walking is involved in this reduction. In previous studies, passive pedaling or manually assisted stepping was used to investigate the effect of afferent input, as it has been technically difficult to eliminate descending inputs from the higher nervous centers during "natural" walking [1,12]. By using these paradigms, Brooke and co-workers found in their series of experiments that the extent of inhibition was dependent on the pedaling velocity [6,12]. Needless to say, however, pedaling and walking are kinetically and kinematically

Abbreviations: AFO, ankle foot orthosis; BF, biceps femoris; BGA, background electromygraphic activity; DGO, driven-gait orthosis; EMG, electromyography; H-reflex, hoffmann reflex; M_{max}, maximum direct motor response; MT, motor threshold; RF, rectus femoris; RMS, root mean square; SCI, spinal cord injury; Sol, soleus; TA, tibialis anterior.

* Corresponding author. Tel.: +81 3 5454 6877; fax: +81 3 5454 6877.
E-mail address: yohei.masugi@gmail.com (Y. Masugi).

http://dx.doi.org/10.1016/j.neulet.2014.10.044
0304-3940/

different. It would be better that the effect of afferent input on the ol H-reflex during walking is studied in passive movements more similar to "natural" walking.

Recently, a passive stepping paradigm with a driven-gait orthosis (DGO; Lokomat®, Hocoma AG, Switzerland) has been used to investigate the effects of afferent input on H-reflex excitability during walking [9,14]. As DGO can support the upright posture of the subjects and impose passive stepping movements that are much similar to "walking," it is useful to elucidate the effects of afferent input during walking without any influence from descending inputs from the higher nervous centers. By using this technique, Kamibayashi et al. found that the Sol H-reflex was reduced during passive stepping with the DGO as compared with during passive standing. As this reduction occurred irrespective of body-weight condition, it was considered that the reduction of the H-reflex was not due to load-related afferent inputs but rather to movement-related afferent inputs from the lower limbs [9]. Taking this result and the series of Brooke et al. into consideration, we hypothesized that the Sol H-reflex during passive stepping would be more reduced as stepping velocity is increased because the amount of movement-related afferent inputs should increase with increasing stepping velocity. The present study was designed to test this hypothesis. Therefore, the purpose of this study is to elucidate the effect of stepping velocity on the Sol H-reflex during robot-assisted stepping.

2. Methods

Eleven healthy male subjects [age, 28 ± 4.9 (SD) years] participated in this study, which was conducted with the approval of the local ethics committee of the national rehabilitation center for persons with disabilities (Saitama, Japan). All subjects participated in the main experiment, and six of them participated in an additional experiment. None of the subjects had any known history of neurological disorders. Each subject provided informed consent to participate in the experimental procedures, which were done in accordance with the Declaration of Helsinki.

A DGO system (Lokomat, Hocoma AG) was used in this study. A detailed description of the device can be found elsewhere [7]. The subjects were fixed into the DGO with a harness around the hip, and cuffs around the legs, and connected to a body-weight support system. To eliminate the effects of load-related afferent inputs, the body weight was fully removed by using an upper body harness that was connected to the DGO system. The feet of the subjectwere not in contact with the ground during passive stepping (called "air stepping"). The knee and hip joints were moved passively from 0° to 60° flexion and from 30° flexion to 15° extension, respectively. As the DGO provided no ankle movements, ankle joints were fixed at neutral position by using ankle foot orthoses (AFOs). The subjects were instructed to relax, and not to intervene with the movements imposed by the DGO during the passive stepping, and practiced the passive stepping task for a few minute before recording. To examine the effect of velocity, passive stepping was performed at five different stride frequencies (14, 21, 28, 35, and 42 min^{-1}). Stride frequency (min^{-1}) was defined as the number of strides per minute. Because the ranges of motions in the lower-limb joints were constant, the stepping velocity was directly related to stride frequency. Electrical stimuli to elicit the H-reflex were delivered at the mid-stance phase of the right leg. In addition to passive stepping, H-reflexes were also recorded during passive standing "in the air." In our preliminary study, we investigated the effect of stepping velocity on the H-reflex at six different phases. The data showed that there were no phase-dependent differences in the modulation of H-reflex with increases in stepping velocity (unpublished data). Therefore, we investigated only a single phase in the current study. There were two reasons why we selected the mid-stance phase of the right leg: (i) as the knee joint is extended at the mid-stance phase, the stimulus efficacy to the nerve is better at this phase than at the other phases; (ii) the position of the right leg at the mid-stance phase is similar to that at a passive standing condition, which we thought was important when H-reflex is compared across different motor tasks or conditions. Each experiment was performed for 2.0–2.5 h.

The electromyographs (EMGs) were recorded from the Sol, tibialis anterior (TA), rectus femoris (RF), and biceps femoris (BF) muscles of the right leg by using bipolar Ag/AgCl surface electrodes (F-150S, 18 × 36 mm; Nihon Kohden, Japan) with an interelectrode distance of 10 mm. The raw EMG signals were amplified (×1000), and band-pass filtered between 15 Hz and 3 kHz by using a bioamplifier system (MEG-6108, Nihon Kohden, Japan). Actual hip and knee joint angular displacements of both orthotic legs were recorded with the DGO potentiometers. All EMG and joint angular signals were digitized at a sampling rate of 5 kHz by using a data acquisition system [Micro1401, Cambridge Electronic Design (CED), UK] and were stored in a computer with Spike2 software (CED).

The Sol H-reflexes were elicited by stimulating the right tibial nerve (rectangular pulse, 1-ms duration) with an electrical stimulator (SEN-7203, Nihon Kohden, Japan), with a cathode (18 × 36 mm) on the popliteal fossa and an anode (50 × 50 mm) placed over the patella. The electrodes were secured with adhesive tape and elastic bands to prevent their movement during the experiment. During passive stepping, an output signal from the DGO system was used as a trigger signal for electrical stimulation. The minimum interstimulus interval was 5 s. The H-reflexes were recorded at the stimulus intensity with an M-wave size of 10% maximal direct motor response (M_{max}) in each condition. H-reflex (n = 12 sweeps) amplitudes were measured during passive standing and stepping at each of the five different velocities. As there was a possibility that the M_{max} would vary across different conditions and over the time course of an experiment [8], the amplitude of M_{max} (n = 3 sweeps) was measured in each condition.

As an additional experiment, the recruitment curves of the M-wave and H-reflex were constructed in 6 of the 11 subjects. The recruitment curves were recorded during passive standing and passive stepping at two different velocity conditions (slow: 14 min^{-1} and fast: 28, 35, or 42 min^{-1}). The stimulus intensity was gradually increased from below the threshold of the H-reflex to above the maximum M-wave, with three stimuli being delivered at each level.

The peak-to-peak amplitudes of the H-reflex, M-wave, and Mmax evoked at each condition were measured offline. To minimize individual variability, the H-reflex and M-wave amplitude were each expressed as a percentage of M_{max} (H/M_{max} and M/M_{max}, respectively). The background electromyographic activity (BGA) levels in the right Sol TA, RF, and BF muscles were determined as the root mean square (RMS) values of the EMG signals for 50 ms before stimulation.

For the analysis of the recruitment curve, the motor threshold (MT) was defined as the lowest stimulus intensity needed to produce an M-wave of 100 μV [11]. The stimulus intensities were expressed as a ratio of MT. The amplitudes of the H-reflex and M-wave were normalized to the corresponding M_{max}. The ascending limb of each individual recruitment curve of the H-reflex was fitted by using the following sigmoid function [10]:

$$H(S) = \frac{H_{max}}{1 + e^{m(S_{50} - S)}} \quad (1)$$

where S is the stimulus intensity, H_{max} is the maximum H-reflex, m is the slope of the function, S_{50} is the stimulus at 50% of the H_{max}, and $H(S)$ is the H-reflex amplitude at a given stimulus value (S).

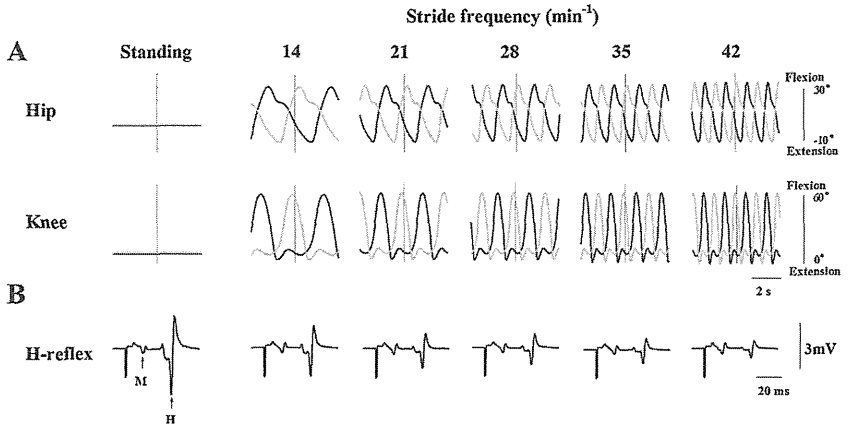

Fig. 1. (A) Typical averaged data (n = 12 sweeps) of right (black lines) and left (gray lines) hip and knee joint angular displacements (°), obtained from a single subject during passive standing and passive stepping at five different velocity conditions (14, 21, 28, 35, and 42 min^{-1}). Each vertical line represents timing of stimulation. (B) Typical averaged data (n = 12 sweeps) of Sol H-reflex waveforms during passive standing and passive stepping at five different velocity conditions.

Hslp was defined as the slope of the ascending limb of the recruitment curve at 50% H_{max}. This slope was determined by using the following equation:

$$\text{Hslp} = \frac{m(H_{max})}{4} \quad (2)$$

The threshold (Hth) of the H-reflex was calculated as the *x*-intercept of the tangent of the function at S_{50}.

Differences in the H/M_{max} and M/M_{max} were tested with a one-way repeated measures analysis of variance (rANOVA) [passive standing and stepping (five different velocity conditions)]. Differences in the H_{max}, Hslp and Hth were also tested with a one-way rANOVA [passive standing and stepping (slow and fast conditions)]. Post hoc Bonferroni tests were used to identify the significant differences among these conditions. Descriptive statistics included mean + standard error of the mean (SEM). For all tests, the level of significance was set at $P < 0.05$.

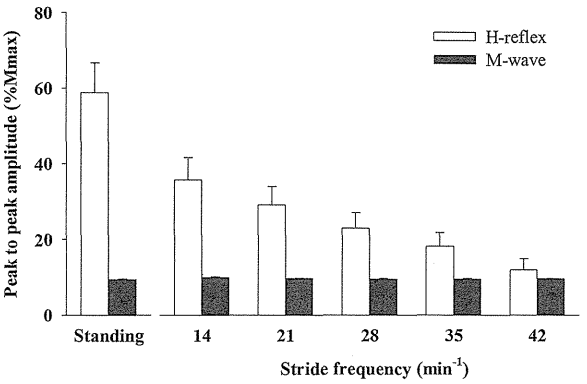

Fig. 2. Peak- to-peak amplitudes of the H-reflex and M-wave in the Sol muscle during passive standing and passive stepping at five different velocity conditions. Filled and open bars represent the average value, and the error bar represents the standard error of the mean (+ SEM) for the 11 subjects.

3. Results

Fig. 1A shows representative hip and knee joint angular displacements (°) during passive standing and during passive stepping at five different velocity conditions, obtained from a single subject. As the hip and knee joint trajectories of the DGO were controlled by a computer, the joint movements were highly repeatable. The stimulus phase was identical across the five different velocity conditions. It was observed that the H-reflexes were inhibited during passive stepping as compared with during passive standing and were decreased with increasing velocity; however, the sizes of the M-wave were the same across different velocity conditions (Fig. 1B).

Fig. 2 shows the mean values (+SEM) of the amplitude of the H-reflex and M-wave for 11 subjects. A one-way rANOVA showed that there was a significant main effect [$F(1.83, 18.33) = 47.37$, $P < 0.001$]. The H-reflexes in each stepping condition were reduced compared with the value at the standing condition (all $P < 0.001$). In the stepping conditions, the H-reflexes were significantly decreased as the

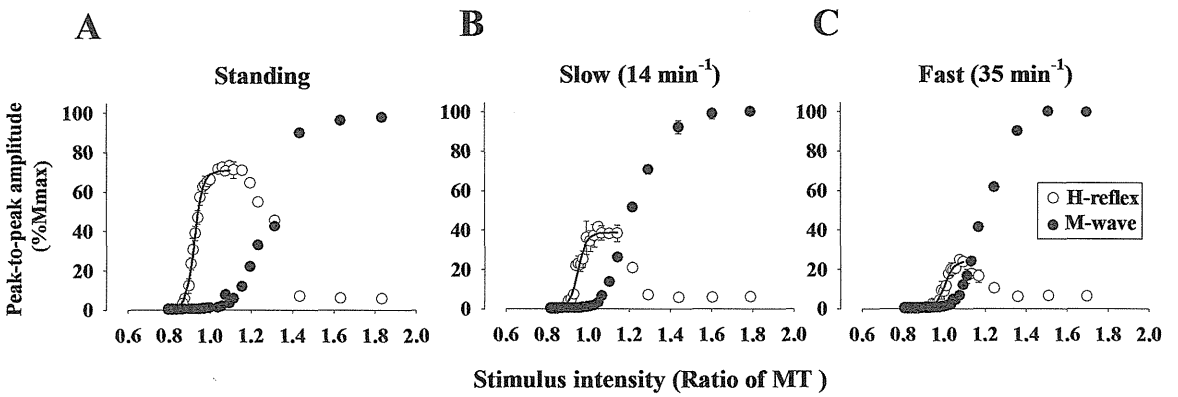

Fig. 3. Examples of recruitment curves of the M-wave and H-reflex during passive standing (A), and stepping at 14 min^{-1} (B), and 35 min^{-1} (C), obtained from a single subject. Each plot shows the mean value of three responses at each stimulus intensity. The sigmoid fitting curves are shown as black lines. MT: motor threshold.

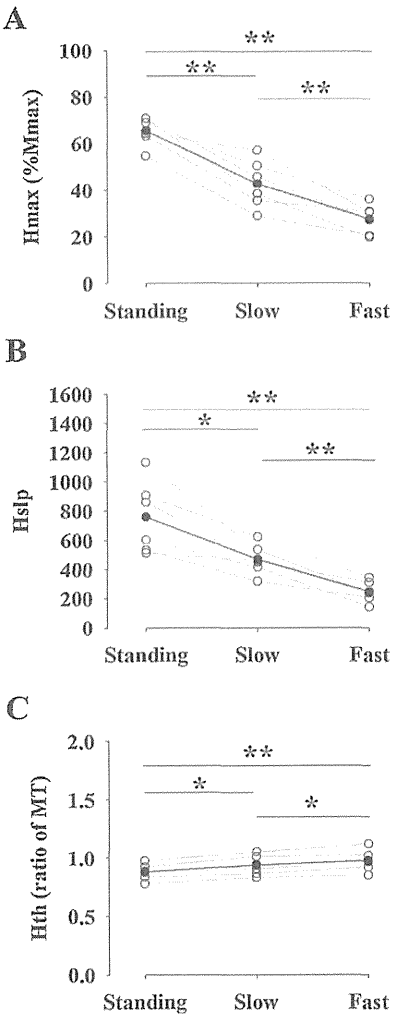

Fig. 4. Three parameters (Hmax, Hslp, and Hth) calculated from the sigmoid function. Filled circles represent the averaged value. Open circles represent the magnitude of the H-reflex in each subject. Significant differences among the three different conditions, $^{*}P < 0.05$, $^{**}P < 0.01$.

stepping velocity increased ($P = 0.001$–0.045), except in the case of 28 vs. 35 min^{-1} ($P = 0.289$) and 35 vs. 42 min^{-1} ($P = 1.02$). As for the M-wave amplitudes, the main effect was not significant [$F(5, 50) = 1.97$, $P = 0.819$]. The BGA levels in the right leg muscles were negligibly small.

Fig. 3 shows the H-reflex recruitment curves during passive standing (A) and passive stepping at slow (B) and fast (C) conditions obtained from a single subject. The maximal H-reflex size was decreased as the velocity increased.

Fig. 4 shows the results for three parameters of the recruitment curves. A one-way rANOVA showed that there was a significant main effect in each parameter [H_{max}: $F(2, 10) = 67.78$, $P < 0.001$, Hslp: $F(2,10) = 26.19$, $P < 0.001$; Hth: $F(2,10) = 40.97$, $P < 0.001$]. The H_{max} (A) and Hslp (B) were significantly smaller in the stepping conditions than in the standing condition ($P < 0.05$). The Hth (C) was significantly higher in the stepping conditions than in the standing condition ($P < 0.05$). Furthermore, H_{max} (A) and Hslp (B) were significantly smaller in the fast stepping condition than in the slow stepping condition ($P < 0.01$). The Hth (C) was significantly higher in the fast stepping condition than in the slow stepping condition ($P < 0.05$).

4. Discussion

The aim of this study was to clarify the effect of stepping velocity on the Sol H-reflex during robot-assisted passive stepping. In this study, passive stepping at five different velocity conditions was provided by the use of a DGO. Our results provide the first demonstration of a velocity-dependent suppression of the Sol H-reflex during passive stepping. The neuronal mechanisms underlying the present results will be discussed below.

In this study, the amplitude of the M-wave elicited in the Sol was used as an index of the consistency of the stimulus intensity, which is an important parameter in human H-reflex experiments involving movements [16]. As no significant main effect was found in M-wave amplitude (M/M_{max}), the afferent volley evoked at each condition was considered to be maintained at a constant level. In addition, as the ankle joint was fixed at the same joint position by using an AFO, there was only little change in Sol muscle geometry with respect to the surface electrodes. To eliminate any influence from the higher nervous centers, the subjects were instructed to relax and not to intervene with the movements imposed by the DGO for passive stepping. As a result, the average BGAs at each velocity were at the noise level, which demonstrated that all subjects were able to achieve the passive stepping. Therefore, the observed changes in the excitability of the Sol H-reflex were most probably due to somatosensory inputs from the lower limbs during passive stepping in the DGO.

In the present study, the H-reflexes were inhibited during passive stepping as compared with during passive standing, and were reduced in size as the stepping velocity increased. During stepping with the DGO, the hip and knee joints were moved passively, whereas the ankle joints were immobilized by using AFOs. As passive stepping was conducted in the air, load-related afferents would not be activated. Therefore, the H-reflex inhibition observed in the present study could be attributed to movement-related afferent inputs from the lower limbs. Furthermore, it was considered that the velocity dependent suppression of the H-reflex was caused by increasing movement-related afferent inputs from the lower limbs, including muscle, joint, cutaneous afferents, etc. In the main experiments, only one stimulus intensity (M-wave size = 10%M_{max}) was used for H-reflex recording to minimize experiment time, although it is better to apply stimulation at various intensities to know the H-reflex excitability in more detail. In additional experiments ($n = 6$), to reveal the input/output relation of the spinal neural circuit mediating H-reflex, we recorded the H-reflex at various stimulus intensities during passive standing and stepping (fast and slow conditions) and constructed the recruitment curves. The characteristics of the curves can be described with three parameters: Hth, Hslp, and Hmax [10]. The changes in the parameters also indicated that the H-reflex excitabilities were more inhibited as the stepping velocity increased (Fig. 4) and provided a more strong evidence of velocity-dependent suppression of the H-reflex during passive stepping.

In previous studies, a passive pedaling or manually assisted stepping has been used to investigate the effect of afferent inputs on the H-reflex during "walking" [1,12]. However, there are differences both in kinematics and kinetics between pedaling and walking. First, the seated posture during pedaling differs from the upright posture during walking. Second, the movement patterns of pedaling differ from that of walking. The DGO used in this study can support the upright posture of the subjects and impose a passive stepping movement that is similar to "natural" walking. In a previous study, Brooke's team reported that H-reflexes were inhibited during passive pedaling as compared with during sitting, and were reduced in size as the pedaling velocity increased [12]. Despite these differences between stepping and pedaling, the present results were consistent with the

results with the pedaling paradigm. Thus, it was considered that the velocity-dependent suppression during passive movements was not related to the posture and movements patterns. Rather, the movement-related somatosensory inputs, which are not context dependent, most probably play the major role in the H-reflex suppression observed during both passive pedaling and stepping. In the series of experiments by Brooke and co-worker they demonstrated that the suppression of the H-reflex during passive pedaling was mainly due to Ia afferent inputs in the knee extensor muscles [4,5,13]. With the present results, we cannot directly identify the source of velocity-dependent suppression of the H-reflex during passive stepping. Although the discharge of different types of sensory receptors in the legs should be increased with increasing velocity, it is considered that, on the basis of the work of Brooke's team, the velocity-dependent suppression during passive stepping might have been due to the increasing discharge rate of Ia afferents.

Concerning the clinical relevance of this study, symptoms of spasticity are often experienced by persons with spinal cord injury (SCI) and are thought to be related to hyper-excitability of the spinal reflex. Furthermore, velocity-dependent modulation is impaired in these patients during walking [15]. In our previous study, we showed that Sol H-reflexes were inhibited during passive stepping as compared with during passive standing, not only in healthy subjects but also in those with clinically motor-complete (SCI) [9]. These results suggest that spinal neural circuits may mediate the Sol H-reflex inhibition during passive stepping, and that there may be a potential therapeutic use for passive stepping (e.g., body-weight supported treadmill training) for the management of spasticity in ankle extensor muscles after SCI and for the improvement of spinal reflex modulations.

Acknowledgements

We thank Hikaru Yokoyama for help and support with the data collection. This work was supported by a Grant-in-Aid for Scientific Research (B) (#23300198) to K. Nakazawa from the Japan Society for the Promotion of Science and by the Ministry of Health, Labor, and Welfare of Japan.

References

[1] J.D. Brooke, J. Cheng, J.E. Misiaszek, K. Lafferty, Amplitude modulation of the soleus H reflex in the human during active and passive stepping movements, J. Neurophysiol. 73 (1995) 102–111.
[2] C. Capaday, R.B. Stein, Amplitude modulation of the soleus H-reflex in the human during walking and standing, J. Neurosci.: Off. J. Soc. Neurosci. 6 (1986) 1308–1313.
[3] C. Capaday, R.B. Stein, Difference in the amplitude of the human soleus H reflex during walking and running, J. Physiol. 392 (1987) 513–522.
[4] J. Cheng, J.D. Brooke, J.E. Misiaszek, W.R. Staines, The relationship between the kinematics of passive movement, the stretch of extensor muscles of the leg and the change induced in the gain of the soleus H reflex in humans, Brain Res. 672 (1995) 89–96.
[5] J. Cheng, J.D. Brooke, W.R. Staines, J.E. Misiaszek, J. Hoare, Long-lasting conditioning of the human soleus H reflex following quadriceps tendon tap, Brain Res. 681 (1995) 197–200.
[6] D.F. Collins, W.E. McIlroy, J.D. Brooke, Contralateral inhibition of soleus H reflexes with different velocities of passive movement of the opposite leg, Brain Res. 603 (1993) 96–101.
[7] G. Colombo, M. Joerg, R. Schreier, V. Dietz, Treadmill training of paraplegic patients using a robotic orthosis, J. Rehabil. Res. Dev. 37 (2000) 693–700.
[8] C. Crone, L.L. Johnsen, H. Hultborn, G.B. Orsnes, Amplitude of the maximum motor response (M_{max}) in human muscles typically decreases during the course of an experiment, Exp. Brain Res. Exp. Hirnforschung. Exp. Cerebrale. 124 (1999) 265–270.
[9] K. Kamibayashi, T. Nakajima, M. Fujita, M. Takahashi, T. Ogawa, M. Akai, K. Nakazawa, Effect of sensory inputs on the soleus H-reflex amplitude during robotic passive stepping in humans, Exp. Brain Res. Exp. Hirnforschung. Exp. Cerebrale. 202 (2010) 385–395.
[10] M. Klimstra, E.P. Zehr, A sigmoid function is the best fit for the ascending limb of the Hoffmann reflex recruitment curve, Exp. Brain Res. Exp. Hirnforschung. Exp. Cerebrale 186 (2008) 93–105.
[11] J.C. Lamy, C. Ho, A. Badel, R.T. Arrigo, M. Boakye, Modulation of soleus H reflex by spinal DC stimulation in humans, J. Neurophysiol. 108 (2012) 906–914.
[12] W.E. McIlroy, D.F. Collins, J.D. Brooke, Movement features and H-reflex modulation. II. Passive rotation, movement velocity and single leg movement, Brain Res. 582 (1992) 85–93.
[13] J.E. Misiaszek, J.K. Barclay, J.D. Brooke, Inhibition of canine H reflexes during locomotor-like rotation about the knee arises from muscle mechanoreceptors in quadriceps, J. Neurophysiol. 73 (1995) 2499–2506.
[14] T. Nakajima, T. Kitamura, K. Kamibayashi, T. Komiyama, E.P. Zehr, S.R. Hundza, K. Nakazawa, Robotic-assisted stepping modulates monosynaptic reflexes in forearm muscles in the human, J. Neurophysiol. 106 (2011) 1679–1687.
[15] C.P. Phadke, F.J. Thompson, C.G. Kukulka, P.M. Nair, M.G. Bowden, S. Madhavan, M.H. Trimble, A.L. Behrman, Soleus H-reflex modulation after motor incomplete spinal cord injury: effects of body position and walking speed, J. Spinal Cord Med. 33 (2010) 371–378.
[16] E.P. Zehr, Considerations for use of the Hoffmann reflex in exercise studies, Eur. J. Appl. Physiol. 86 (2002) 455–468.

Published OnlineFirst January 14, 2015; DOI: 10.1158/1078-0432.CCR-14-2775

Personalized Medicine and Imaging

Clinical Cancer Research

Potential Role of pNF-H, a Biomarker of Axonal Damage in the Central Nervous System, as a Predictive Marker of Chemotherapy-Induced Cognitive Impairment

Akina Natori[1], Toru Ogata[2], Masahiko Sumitani[3], Takamichi Kogure[3], Teruo Yamauchi[1], and Hideko Yamauchi[4]

Abstract

Purpose: Chemotherapy-induced cognitive impairment (CICI) is a clinically significant problem. Previous studies using magnetic resonance imaging indicated structural changes in the cerebral white matter of patients with CICI. Phosphorylated neurofilament heavy subunit (pNF-H), a major structural protein in axons, was recently reported to be elevated in the serum of patients with some central nervous system disorders. We performed a cross-sectional analysis of neuropsychological test results and serum pNF-H levels in patients undergoing adjuvant chemotherapy for breast cancer. Our hypothesis was that CICI is accompanied by axonal damage that can be detected by elevated serum pNF-H levels.

Experimental Design: Seventy-six patients with early breast cancer in various phases of treatment (naïve to chemotherapy; after one, three, or seven cycles of chemotherapy; or with a history of chemotherapy) were assessed by self-administered neuropsychological tests and a single pNF-H measurement. The χ^2 and Mann–Whitney tests were used for statistical analysis.

Results: Increased pNF-H levels were observed in 28.8% of the patients who underwent chemotherapy, but in none of the chemotherapy-naïve patients or patients with a history of chemotherapy. The pNF-H–positive rate increased significantly in proportion to the number of chemotherapy cycles (one cycle, 5.0%; three cycles, 31.6%; seven cycles, 55.0%; $P < 0.05$). No significant differences in neuropsychological test results were observed among the groups.

Conclusions: The serum pNF-H level in patients undergoing chemotherapy for breast cancer increased in a cumulative dose-dependent manner, suggesting its potential application as a biomarker of neural damage after chemotherapy. *Clin Cancer Res; 21(6); 1348–52. ©2015 AACR.*

Introduction

Chemotherapy can offer long-term survival for patients with cancer, especially patients with breast cancer and blood cancer. However, several recent reports (1–3) have revealed that chemotherapy may induce cognitive dysfunction such as deficits in attention, concentration, executive function, verbal or visual learning, and processing speed (4, 5) For example, one study showed that patients' attention and memory task abilities were worse after than before chemotherapy. However, healthy subjects exhibited progressive improvement in these abilities with task repetition (6). Although the cognitive dysfunction following chemotherapy is usually less severe, it sometimes impairs activities of daily living and quality of life to the point of debilitation. Recently, such chemotherapy-induced cognitive impairment (CICI) has been recognized as a clinically significant issue in patients treated with chemotherapy and cancer survivors with a history of chemotherapy (1–3, 7–9). Elucidation of the mechanisms of and diagnostic and therapeutic measures for CICI is urgently required.

One proposed mechanism of CICI is direct neurotoxicity by chemotherapy itself (7). Magnetic resonance imaging studies have demonstrated lower integrity of cerebral white matter (location of myelinated axons) rather than gray matter (location of neuronal cell bodies) in patients with CICI than in healthy subjects (10–12). However, these findings do not directly indicate whether the decreased integrity of the cerebral white matter is caused by damage to axons themselves, which are the main components of white matter, or by Wallerian axonal degeneration following neuronal damage.

Various tissues in the central nervous system (CNS), including neurons, axons, and glia, release several lines of proteins into the cerebral spinal fluid and/or peripheral blood flow when damaged (13–17). The use of some of these proteins in the cerebral spinal fluid and/or blood has been explored as objective biomarkers of the severity of neuronal damage. Increased levels of the circulating phosphorylated form of the high-molecular-weight neurofilament subunit (pNF-H), a major structural protein in central and

[1]Division of Medical Oncology, Department of Internal Medicine, St. Luke's International Hospital, Tokyo, Japan. [2]Research Institute, National Rehabilitation Center for Persons with Disabilities, Tokorozawa City, Japan. [3]Department of Pain and Palliative Medicine, The University of Tokyo Hospital, Tokyo, Japan. [4]Department of Breast Surgery, St. Luke's International Hospital, Tokyo, Japan.

Corresponding Author: Hideko Yamauchi, Department of Breast Surgery, St. Luke's International Hospital, 9-1 Akashi-cho, Chuo-ku, Tokyo 104-8560, Japan. Phone: 81-3-3541-5151; Fax: 81-3-5550-2624; E-mail: hideyama@luke.ac.jp

doi: 10.1158/1078-0432.CCR-14-2775

Published OnlineFirst January 14, 2015; DOI: 10.1158/1078-0432.CCR-14-2775

Translational Relevance

Chemotherapy-induced cognitive impairment (CICI) has been recognized as a clinically significant issue in patients treated with chemotherapy and cancer survivors with a history of chemotherapy. Elucidation of the mechanisms of and diagnostic and therapeutic measures for CICI is urgently required. This study investigated CICI with a particular focus on the phosphorylated form of the high-molecular-weight neurofilament heavy subunit NF-H (pNF-H), a major structural protein in axons, as a predictive maker of CICI. We found that the serum pNF-H level in patients undergoing chemotherapy for breast cancer increased in a cumulative dose-dependent manner, suggesting the potential application of pNF-H as a biomarker of neural damage after chemotherapy. It might be useful to investigate the mechanisms and severity indexes of CICI and neuronal toxicity of chemotherapy on the CNS by using pNF-H as a surrogate marker, rather than subjective cognitive test batteries.

peripheral axons, were recently reported in a rodent model of spinal cord injury (17). The pNF-H level is associated with the severity of spinal cord injury (18) and may have adequate sensitivity to serve as a biomarker of treatment efficacy in patients with spinal cord injury (19). Increased pNF-H levels are also observed in patients with supraspinal CNS damage, such as that caused by multiple sclerosis (20), febrile seizures (21), hypoxic-ischemic encephalopathy (22), acute intracerebral hemorrhage, and other conditions. Thus, pNF-H has potential as an effective biomarker of CNS damage caused by either neuronal or axonal injury.

The purpose of the present study was to evaluate the potential role of pNF-H as a predictive marker of CICI. We performed a cross-sectional analysis of the results of neuropsychological tests, which can be conducted in the clinical setting and serum pNF-H levels in patients with breast cancer undergoing adjuvant chemotherapy.

Patients and Methods

Patients

Patients were eligible if they had histologic proof of early breast cancer. Patients were ineligible if they were <18 or >70 years of age, had a psychiatric disorder, or had a history of chemotherapy for another malignancy. The patients were assigned to various phases of treatment (before chemotherapy, after one cycle of chemotherapy, after three cycles of chemotherapy, after seven cycles of chemotherapy, and survivors who had undergone previous chemotherapy). Both neoadjuvant and adjuvant chemotherapy were eligible for inclusion. Various chemotherapy regimens were acceptable. The use of hormone agents was permitted in the group of patients who had undergone previous chemotherapy. These hormone agents including both tamoxifen and aromatase inhibitors were applied to the patients according to their menopausal status. Written informed consent was obtained from all participants. This study was approved by the institutional review board of our hospital and supported by Health Labour Sciences Research Grant from the Japanese Ministry of Health, Labour and Welfare (H24-Ganrinsho-ippan-011 and H26-Kakushinntekigan-ippan-060).

Methods

All patients underwent self-administered neuropsychological tests and pNF-H level measurements at once when they were assigned. The EuroQOL-5 Dimension questionnaire (EQ-5D), Hospital Anxiety and Depression Scale (HAD), State-Trait Anxiety Inventory (STAI), PainDETECT questionnaire, Epworth Sleepiness Scale (ESS), Raven's Colored Progressive Matrices (RCPM), Cognitive Failure Questionnaire (CFQ), Japanese version of the Brief Fatigue Inventory (BFI-J), Japanese version of the Newest Vital Sign (NVS-J), and Japanese Adult Reading Test (JART) were used. The EQ-5D is a scale of health-related quality of life (23), and the HAD is a self-assessment scale of anxiety and depression in the setting of an outpatient clinic of a medical hospital (24). The STAI is a 40-item instrument that measures transient and enduring levels of anxiety (25). PainDETECT is a screening questionnaire used to identify peripheral neuropathy and neuropathic pain (26). The ESS is a scale of subjective sleepiness (27). The RCPM is a standardized test designed to measure nonverbal intellectual capacity (28). The CFQ assesses self-reported cognitive functioning (29). The BFI-J is a nine-item questionnaire designed to assess fatigue in patients with cancer (30, 31). The NVS-J measures health literacy in Japanese adults (32). The JART evaluates the premorbid intelligence quotient (33). The serum pNF-H level was determined with a commercially available enzyme-linked immunosorbent assay kit (Human Phosphorylated Neurofilament H ELISA; BioVendor), following the manufacturer's protocol. The serum samples were diluted 3-fold before the analysis. pNF-H levels of >70.5 pg/mL were considered to be positive (18).

All statistical analyses were performed using SPSS software. The χ^2 and Mann–Whitney tests were used to compare data. Statistical significance was assessed at $P < 0.05$.

Results

A total of 76 patients participated in this study. Five patients were naïve to chemotherapy; 20 had completed 1 cycle of chemotherapy, 20 had completed 3 cycles of chemotherapy, 19 had completed 7 cycles of chemotherapy, and 12 had completed chemotherapy at least 24 months before this study. The patients' demographic data and neuropsychological test results are summarized in Tables 1 and 2. An increased pNF-H level was observed in 28.8% of the patients who underwent chemotherapy, but in none of the chemotherapy-naïve patients or patients who had undergone previous chemotherapy. The pNF-H–positive rate in each patient group treated with chemotherapy increased significantly in proportion to the number of chemotherapy cycles (one cycle, 5.0%; three cycles, 31.6%; seven cycles, 55.0%; $P < 0.05$; Fig. 1). The average pain intensity in each group according to the PainDETECT was 3.0 ± 2.3, 1.8 ± 1.8, 1.7 ± 2.0, 1.6 ± 1.6, and 1.6 ± 1.9 (naïve to chemotherapy, after one cycle of chemotherapy, after three cycles of chemotherapy, after seven cycles of chemotherapy, and previously treated by chemotherapy, respectively; $P = 0.65$). The PainDETECT numbness scores in each group were 2.2 ± 1.3, 1.2 ± 0.4, 2.0 ± 1.0, 1.6 ± 1.1, and 1.8 ± 0.8, respectively ($P = 0.14$). Symptoms of peripheral neuropathy in the patients with increasing pNF-H levels were not salient and were comparable with those in pNF-H–negative patients. The average PainDETECT pain intensity and numbness scores in the pNF-H–positive versus pNF-H–negative patients were 1.6 ± 1.8 versus 1.8 ± 1.8 ($P = 0.62$) and 1.5 ±

Published OnlineFirst January 14, 2015; DOI: 10.1158/1078-0432.CCR-14-2775

Table 1. Patient demographics

	Chemotherapy naïve ($N = 5$)	After 1 cycle of chemotherapy ($N = 20$)	After 3 cycles of chemotherapy ($N = 20$)	After 7 cycles of chemotherapy ($N = 19$)	Patients with a history of previous chemotherapy ($N = 12$)
Age (median), y	49	45.5	45	50	46
Postmenopausal, *n* (%)	3 (60)	3 (15)	9 (45)	7 (35)	6 (50)
Hormonal therapy, *n* (%)	0 (0)	0 (0)	0 (0)	0 (0)	9 (75)
Chemotherapy regimen, *n* (%)					
FEC	N/A	1 (5)	4 (20)	N/A	N/A
AC	N/A	15 (75)	9 (45)	N/A	N/A
DOC	N/A	4 (20)	7 (35)	N/A	N/A
FEC-DOC	N/A	N/A	N/A	15 (79)	8 (67)
AC-DOC	N/A	N/A	N/A	3 (16)	0 (0)
Other	N/A	N/A	N/A	1 (5)	4 (33)
Days from first chemotherapy (median)	N/A	21	63	154	944

Abbreviations: AC, adriamycin and cyclophosphamide; DOC, docetaxel; FEC, 5-fluorouracil, epirubicin, and cyclophosphamide; N/A, not applicable.

1.1 versus 1.7 ± 0.9 ($P = 0.18$), respectively. No significant differences were observed in the neuropsychological test results among the patient groups (Table 3).

Discussion

In the present study, some of the patients treated with chemotherapy showed increased serum pNF-H levels, and the chemotherapy-associated pNF-H positivity rate increased in a cumulative dose-dependent manner. These findings indicate that the serum pNF-H level in patients treated with chemotherapy is probably derived from axon degeneration in the CNS and that neuronal toxicity by chemotherapy operates temporally because none of the patients who had completed chemotherapy at least 24 months before the study showed increasing pNF-H levels. These results suggest a potential application of pNF-H as a biomarker of neural damage in the CNS after chemotherapy. In patients with chemotherapy-induced peripheral neuropathy, it is already known that chemotherapy impairs function of the peripheral nervous system in a cumulative dose-dependent manner (34, 35). However, among the present study participants, few patients showed peripheral neuropathy and neuropathic pain, and cumulative dose-dependent development of neuropathy was not observed. Furthermore, although pNF-H is certainly included in the peripheral nerve axon and oxaliplatin can lead to loss of pNF-H immunoreactivity in the dorsal root ganglion (36), symptoms of peripheral neuropathy with increasing pNF-H levels were not salient in the present patients, as in pNF-H–negative patients.

We found no differences in the neuropsychological test results between patients with and without increasing pNF-H levels. These tests failed to detect cognitive decline from the pretreatment to posttreatment period in almost all of the patients who still scored within the normal range in the posttreatment period, possibly because of high premorbid cognitive function. Previous studies (6, 10, 11) used more dedicated cognitive test batteries assessed by an experimenter, and the tests were applied much later than in the present study. The time points at which the patients were assessed by neuropsychological tests vary among previous studies, but many tests were conducted from 1 month to 1 year after

Table 2. Results of neuropsychological tests among groups sorted by treatment phase

	Chemotherapy naïve ($N = 5$)	After 1 cycle of chemotherapy ($N = 20$)	After 3 cycles of chemotherapy ($N = 20$)	After 7 cycles of chemotherapy ($N = 19$)	Patients with a history of previous chemotherapy ($N = 12$)
pNF-H–positive, *n* (%)	0 (0)	1 (5)	6 (30)	11 (57.8)	0 (0)
CFQ[a] (mean, SD)	21.5 ± 8.3	19.4 ± 11.0	17.5 ± 10.8	18.4 ± 11.4	25.6 ± 10.9
HADS[b]					
Anxiety subscale (mean, SD)	5.0 ± 2.9	5.5 ± 2.8	3.7 ± 2.8	5.0 ± 2.9	4.3 ± 2.9
Depression subscale (mean, SD)	3.4 ± 4.0	4.7 ± 3.4	3.9 ± 3.4	4.0 ± 3.6	2.8 ± 3.4
STAI[b]					
State anxiety (mean, SD)	41.6 ± 11.6	43.3 ± 11.1	38.3 ± 11.4	42.0 ± 11.9	36.9 ± 11.2
Trait anxiety (mean, SD)	45 ± 9.8	44.9 ± 11.4	35.0 ± 11.4	42.7 ± 11.9	38.1 ± 11.2
ESS[b] (mean, SD)	6.6 ± 4.0	10.5 ± 4.2	9.2 ± 4.1	8.0 ± 3.8	8.8 ± 3.8
BFI-J[b] (mean, SD)	34.5 ± 17.5	16 ± 14.8	16.3 ± 14.7	17.3 ± 15.8	21.9 ± 15.7
NVS[a] (mean, SD)	4.6 ± 0.7	4.2 ± 1.1	4.5 ± 1.1	4.6 ± 1.2	4.2 ± 1.1
JART[a] (mean, SD)					
Full-scale IQ	109.6 ± 7.5	106.7 ± 9.4	110.5 ± 9.2	110.2 ± 10.0	110.9 ± 9.6
Verbal IQ	111.4 ± 8.6	108.1 ± 10.6	112.4 ± 10.5	112.1 ± 11.3	112.8 ± 10.9
Performance IQ	106.3 ± 5.5	104.2 ± 6.9	107.0 ± 6.8	106.8 ± 7.3	107.2 ± 7.1
RCPM[a] (mean, SD)	36.0 ± 1.3	36.0 ± 0.7	35.8 ± 0.7	35.8 ± 0.8	35.5 ± 0.7
PainDETECT[b] (mean, SD)	4.1 ± 4.7	4.0 ± 4.8	3.7 ± 4.7	4.2 ± 5.0	4.2 ± 4.7
EQ5D[a] (mean, SD)	0.8 ± 0.1	0.8 ± 0.1	0.8 ± 0.1	0.8 ± 0.1	0.8 ± 0.1

Abbreviations: CFQ, cognitive failure questionnaire; EQ5D, EuroQOL-5 Dimension questionnaire; HADS, Hospital Anxiety and Depression Scale; IQ, intelligence quotient; pNF-H, phosphorylated form of the high-molecular-weight neurofilament subunit.

[a]The score would decrease when the function declines.

[b]The score would increase when the function declines.

Published OnlineFirst January 14, 2015; DOI: 10.1158/1078-0432.CCR-14-2775

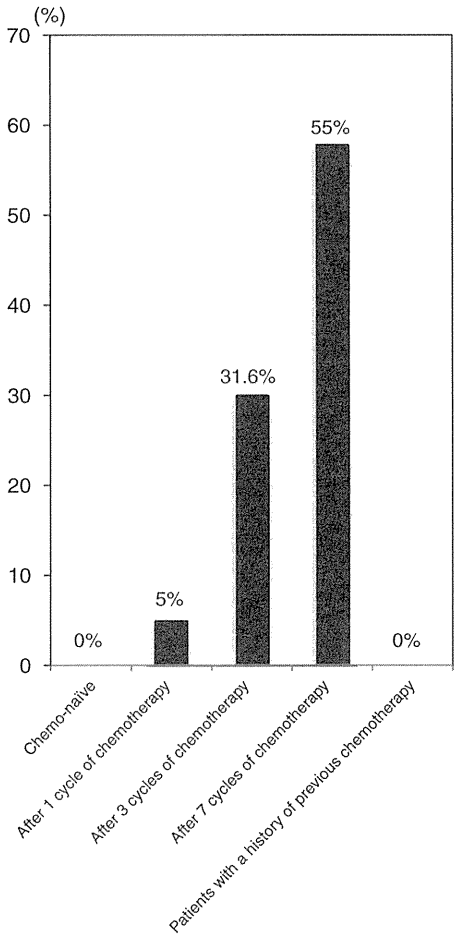

Figure 1.
Rate of pNF-H positivity in each patient group treated with chemotherapy. pNF-H, phosphorylated form of the high-molecular-weight neurofilament subunit.

chemotherapy (3, 10–12, 37). We used self-administered neuropsychological tests to screen CICI in common clinical settings using simple cognitive test batteries. However, such tests might not be sensitive enough to detect subtle changes in CICI. Whether intimate relationships exist between the pNF-H level and dedicated cognitive test batteries requires further assessment. Subjective complaints regarding cognitive decline after chemotherapy and other cancer treatments might be associated with depression, anxiety, and fatigue (2, 3). Most of the participants in the present study showed no depression or anxiety. Moreover, the cognitive decline was not found among the patients who went into menopause or used some hormonal therapy, although menopausal status and hormone therapy might affect the cognitive function (38). These may have been related to the fact that the neuropsychological test results did not detect cognitive decline. It might be useful to investigate the mechanisms and severity indices of CICI and neural toxicity of chemotherapy on the CNS using pNF-H as a surrogate marker rather than subjective cognitive test batteries.

Table 3. Results of neuropsychological tests among groups sorted by pNF-H level

	pNF-H–positive ($N = 18$)	pNF-H–negative ($N = 56$)	*P*
CFQ[a] (mean, SD)	18.8 ± 11.2	21.1 ± 10.6	0.77
HADS[b]			
Anxiety subscale (mean, SD)	4.3 ± 2.8	4.9 ± 2.8	0.35
Depression subscale (mean, SD)	4.5 ± 3.5	3.9 ± 3.3	0.83
STAI[b]			
State anxiety (mean, SD)	40.1 ± 11.2	42.8 ± 10.9	0.79
Trait anxiety (mean, SD)	40.2 ± 11.3	43.1 ± 11.2	0.41
ESS[b] (mean, SD)	8.5 ± 4.2	9.5 ± 4.1	0.26
BFI-J[b] (mean, SD)	18.1 ± 14.4	19.1 ± 14.9	0.74
NVS[a] (mean, SD)	4.8 ± 1.2	4.5 ± 1.1	0.18
JART[a]			
Full-scale IQ (mean, SD)	110.4 ± 9.3	113.4 ± 9.3	0.79
Verbal IQ (mean, SD)	112.3 ± 10.6	115.2 ± 10.6	0.79
Performance IQ (mean, SD)	107.0 ± 6.8	110.1 ± 6.8	0.79
RCPM[a] (mean, SD)	35.9 ± 0.7	37.0 ± 0.7	0.37
PainDETECT[b] (mean, SD)	4.2 ± 4.9	4.1 ± 4.7	0.26
EQ5D[b] (mean, SD)	0.8 ± 0.1	0.8 ± 0.1	0.87

Abbreviations: CFQ, cognitive failure questionnaire; EQ5D, EuroQOL-5 Dimension questionnaire; HADS, Hospital Anxiety and Depression Scale; IQ, intelligence quotient; pNF-H, phosphorylated form of the high-molecular-weight neurofilament subunit.
[a]The score would decrease when the function declines.
[b]The score would increase when the function declines.

Conclusions

The serum pNF-H level in patients with breast cancer treated with chemotherapy increased in a cumulative dose-dependent manner. Axonal damage in the CNS can be cumulatively caused by chemotherapy, which might eventually lead to CICI. The present findings suggest a potential application of pNF-H as a biomarker of CNS damage after chemotherapy. However, the self-administered neuropsychological tests used in this study did not demonstrate significant cognitive impairment. A prospective cohort study is needed to validate the usefulness of pNF-H for assessment of CICI.

Disclosure of Potential Conflicts of Interest

No potential conflicts of interest were disclosed.

Authors' Contributions

Conception and design: A. Natori, M. Sumitani, T. Yamauchi, H. Yamauchi
Development of methodology: A. Natori, T. Ogata, T. Kogure, T. Yamauchi, H. Yamauchi
Acquisition of data (provided animals, acquired and managed patients, provided facilities, etc.): A. Natori, T. Ogata, T. Yamauchi, H. Yamauchi
Analysis and interpretation of data (e.g., statistical analysis, biostatistics, computational analysis): A. Natori, M. Sumitani, T. Kogure, T. Yamauchi, H. Yamauchi
Writing, review, and/or revision of the manuscript: A. Natori, T. Kogure, T. Yamauchi, H. Yamauchi
Administrative, technical, or material support (i.e., reporting or organizing data, constructing databases): A. Natori, T. Yamauchi, H. Yamauchi
Study supervision: H. Yamauchi

Grant Support

This study was supported by Health Labour Sciences Research Grant from the Japanese Ministry of Health, Labour and Welfare (H24-Ganrinsho-ippan-011 and H26-Kakushinntekigan-ippan-060).

The costs of publication of this article were defrayed in part by the payment of page charges. This article must therefore be hereby marked *advertisement* in accordance with 18 U.S.C. Section 1734 solely to indicate this fact.

Received October 27, 2014; revised December 13, 2014; accepted December 31, 2014; published OnlineFirst January 14, 2015.

Published OnlineFirst January 14, 2015; DOI: 10.1158/1078-0432.CCR-14-2775

References

1. Jim HSL, Phillips KM, Chait S, Faul LA, Popa MA, Lee Y-H, et al. Meta-analysis of cognitive functioning in breast cancer survivors previously treated with standard-dose chemotherapy. J Clin Oncol 2012;30:3578–87.
2. O'Farrell E, MacKenzie J, Collins B. Clearing the air: a review of our current understanding of "chemo fog." Curr Oncol Rep 2013;15:260–9.
3. Collins B, Mackenzie J, Stewart A, Bielajew C, Verma S. Cognitive effects of chemotherapy in post-menopausal breast cancer patients 1 year after treatment. Psycho Oncol 2009;18:134–43.
4. Wefel JS, Witgert ME, Meyers CA. Neuropsychological sequelae of non-central nervous system cancer and cancer therapy. Neuropsychol Rev 2008;18:121–31.
5. Correa DD, Ahles TA. Neurocognitive changes in cancer survivors. Cancer J 2008;14:396–400.
6. Collins B, MacKenzie J, Tasca GA, Scherling C, Smith A. Cognitive effects of chemotherapy in breast cancer patients: a dose-response study. Psychooncology 2013;22:1517–27.
7. Ahles TA, Saykin AJ. Candidate mechanisms for chemotherapy-induced cognitive changes. Nat Rev Cancer 2007;7:192–201.
8. Wefel JS, Vardy J, Ahles T, Schagen SB. International Cognition and Cancer Task Force recommendations to harmonise studies of cognitive function in patients with cancer. Lancet Oncol 2011;12:703–8.
9. Silverman DH, Dy CJ, Castellon SA, Lai J, Pio BS, Abraham L, et al. Altered frontocortical, cerebellar, and basal ganglia activity in adjuvant-treated breast cancer survivors 5–10 years after chemotherapy. Breast Cancer Res Treat 2007;103:303–11.
10. Deprez S, Amant F, Yigit R, Porke K, Verhoeven J, Van den Stock J, et al. Chemotherapy-induced structural changes in cerebral white matter and its correlation with impaired cognitive functioning in breast cancer patients. Hum Brain Mapp 2011;32:480–93.
11. Deprez S, Amant F, Smeets A, Peeters R, Leemans A, Van Hecke W, et al. Longitudinal assessment of chemotherapy-induced structural changes in cerebral white matter and its correlation with impaired cognitive functioning. J Clin Oncol 2012;30:274–81.
12. Inagaki M, Yoshikawa E, Matsuoka Y, Sugawara Y, Nakano T, Akechi T, et al. Smaller regional volumes of brain gray and white matter demonstrated in breast cancer survivors exposed to adjuvant chemotherapy. Cancer 2007;109:146–56.
13. Loy DN, Sroufe AE, Pelt JL, Burke DA, Cao QL, Talbott JF, et al. Serum biomarkers for experimental acute spinal cord injury: rapid elevation of neuron-specific enolase and S-100beta. Neurosurgery 2005;56:391–7; discussion 7.
14. Cao F, Yang XF, Liu WG, Hu WW, Li G, Zheng XJ, et al. Elevation of neuron-specific enolase and S-100beta protein level in experimental acute spinal cord injury. J Clin Neurosci 2008;15:541–4.
15. Pouw MH, Hosman AJ, van Middendorp JJ, Verbeek MM, Vos PE, van de Meent H. Biomarkers in spinal cord injury. Spinal Cord 2009;47:519–25.
16. Kwon BK, Stammers AM, Belanger LM, Bernardo A, Chan D, Bishop CM, et al. Cerebrospinal fluid inflammatory cytokines and biomarkers of injury severity in acute human spinal cord injury. J Neurotrauma 2010;27:669–82.
17. Shaw G, Yang C, Ellis R, Anderson K, Parker Mickle J, Scheff S, et al. Hyperphosphorylated neurofilament NF-H is a serum biomarker of axonal injury. Biochem Biophys Res Commun 2005;336:1268–77.
18. Hayakawa K, Okazaki R, Ishii K, Ueno T, Izawa N, Tanaka Y, et al. Phosphorylated neurofilament subunit NF-H as a biomarker for evaluating the severity of spinal cord injury patients, a pilot study. Spinal Cord 2012;50:493–6.
19. Ueno T, Ohori Y, Ito J, Hoshikawa S, Yamamoto S, Nakamura K, et al. Hyperphosphorylated neurofilament NF-H as a biomarker of the efficacy of minocycline therapy for spinal cord injury. Spinal Cord 2011;49:333–6.
20. Gresle MM, Liu Y, Dagley LF, Haartsen J, Pearson F, Purcell AW, et al. Serum phosphorylated neurofilament-heavy chain levels in multiple sclerosis patients. J Neurol Neurosurg Psychiatry 2014;85:1209–13.
21. Matsushige T, Inoue H, Fukunaga S, Hasegawa S, Okuda M, Ichiyama T. Serum neurofilament concentrations in children with prolonged febrile seizures. J Neurol Sci 2012;321:39–42.
22. Douglas-Escobar M, Weiss MD. Biomarkers of hypoxic-ischemic encephalopathy in newborns. Front Neurol 2012;3:144.
23. EuroQol Group. EuroQol—a new facility for the measurement of health-related quality of life. Health Policy 1990;16:199–208.
24. Zigmond AS, Snaith RP. The hospital anxiety and depression scale. Acta Psychiatr Scand 1983;67:361–70.
25. Spielberger CD, Gorsuch RL, Lushene R, Vagg PR, Jacobs GA. Manual for the state-trait anxiety inventory. Palo Alto, CA: Consulting Psychologists Press; 1983.
26. Freynhagen R, Baron R, Gockel U, Tolle TR. painDETECT: a new screening questionnaire to identify neuropathic components in patients with back pain. Curr Med Res Opin 2006;22:1911–20.
27. Johns MW. A new method for measuring daytime sleepiness: the Epworth sleepiness scale. Sleep 1991;14:540–5.
28. Raven JC. Colored progressive matrices sets A, Ab, B. Oxford: Oxford Psychologists Press Ltd.; 1947, 1995.
29. Broadbent DE, Cooper PF, FitzGerald P, Parkes KR. The cognitive failures questionnaire (CFQ) and its correlates. Br J Clin Psychol 1982;21:1–16.
30. Mendoza TR, Wang XS, Cleeland CS, Morrissey M, Johnson BA, Wendt JK, et al. The rapid assessment of fatigue severity in cancer patients: use of the brief fatigue inventory. Cancer 1999;85:1186–96.
31. Okuyama T, Wang XS, Akechi T, Mendoza TR, Hosaka T, Cleeland CS, et al. Validation study of the Japanese version of the brief fatigue inventory. J Pain Symptom Manage 2003;25:106–17.
32. Powers BJ, Trinh JV, Bosworth HB. Can this patient read and understand written health information? JAMA 2010;304:76–84.
33. Matsuoka K, Uno M, Kasai K, Koyama K, Kim Y. Estimation of premorbid IQ in individuals with Alzheimer's disease using Japanese ideographic script (Kanji) compound words: Japanese version of national adult reading test. Psychiatry Clin Neurosci 2006;60:332–9.
34. Cavaletti G, Cornblath DR, Merkies ISJ, Postma TJ, Rossi E, Frigeni B, et al. The chemotherapy-induced peripheral neuropathy outcome measures standardization study: from consensus to the first validity and reliability findings. Ann Oncol 2013;24:454–62.
35. Stubblefield MD, Burstein HJ, Burton AW, Custodio CM, Deng GE, Ho M, et al. NCCN task force report: management of neuropathy in cancer. J Natl Compr Canc Netw 2009;7:S1–S26.
36. Jamieson SM, Subramaniam J, Liu JJ, Jong NN, Ip V, Connor B, et al. Oxaliplatin-induced loss of phosphorylated heavy neurofilament subunit neuronal immunoreactivity in rat DRG tissue. Mol Pain 2009;5:66.
37. McDonald BC, Conroy SK, Ahles TA, West JD, Saykin AJ. Gray matter reduction associated with systemic chemotherapy for breast cancer: a prospective MRI study. Breast Cancer Res Treat 2010;123:819–28.
38. Collins B, Mackenzie J, Stewart A, Bielajew C, Verma S. Cognitive effects of hormonal therapy in early stage breast cancer patients: a prospective study. Psychooncology 2009;18:811–21.

Published OnlineFirst January 14, 2015; DOI: 10.1158/1078-0432.CCR-14-2775

AACR American Association for Cancer Research

Clinical Cancer Research

Potential Role of pNF-H, a Biomarker of Axonal Damage in the Central Nervous System, as a Predictive Marker of Chemotherapy-Induced Cognitive Impairment

Akina Natori, Toru Ogata, Masahiko Sumitani, et al.

Clin Cancer Res 2015;21:1348-1352. Published OnlineFirst January 14, 2015.

Spinal Cord (2015), 1–8

www.nature.com/sc

ORIGINAL ARTICLE

Mechanical and neural changes in plantar-flexor muscles after spinal cord injury in humans

K Yaeshima[1,2], D Negishi[3], S Yamamoto[3], T Ogata[2], K Nakazawa[1] and N Kawashima[2]

Study design: Cross-sectional study.
Objectives: To determine the effect of injury duration on plantar-flexor elastic properties in individuals with chronic spinal cord injury (SCI) and spasticity.
Setting: National Rehabilitation Center for Persons with Disabilities, Japan.
Methods: A total of 16 chronic SCI patients (age, 33 ± 9.3 years; injury localization, C6-T12; injury duration, 11–371 months) participated. Spasticity of the ankle plantar-flexors was assessed using the Modified Ashworth Scale (MAS). The calf circumference and muscle thickness of the medial gastrocnemius (MG), lateral gastrocnemius and soleus were assessed using tape measure and ultrasonography. In addition, the ankle was rotated from 10° plantar-flexion to 20° dorsiflexion at 5 deg s^{-1} with a dynamometer, and the ankle angle and torque were recorded. After normalizing the data (the initial points of angle and torque were set to zero), we calculated the peak torque and energy. Furthermore, angle–torque data (before and after normalization) were fitted with a second- and fourth-order polynomial, and exponential (Sten–Knudsen) models, and stiffness indices (SI_{SOP}, SI_{FOP}, SI_{SK}) and $Angle_{SLACK}$ (the angle at which plantar-flexor passive torque equals zero) were calculated. The stretch reflex gain and offset were determined from 0–10° dorsiflexion at 50, 90, 120 and 150 deg s^{-1}. After logarithmic transformation, Pearson's correlation coefficients were calculated.
Results: MAS, calf circumference, MG thickness, peak torque and SI_{FOP} significantly decreased with injury duration (r log-log = −0.63, −0.69, −0.63, −0.53 and −0.55, respectively, $P<0.05$). The peak torque and SI_{FOP} maintained significant relationships even after excluding impacts from muscle morphology.
Conclusion: Plantar-flexor elasticity in chronic SCI patients decreased with increased injury duration.
Spinal Cord advance online publication, 10 February 2015; doi:10.1038/sc.2015.9

INTRODUCTION

Motor paralysis following spinal cord injury (SCI) inevitably prevents daily activities such as upright standing and bipedal walking; consequently, physical activity declines in affected patients. Previous studies have indicated that SCI patients experience extreme muscle atrophy,[1–3] fiber transformation towards a fast-fatigable type[4–6] and decreased bone mineral density.[7,8] This musculoskeletal degeneration is attributed largely to the dramatically decreased muscle activity and mechanical stress in the paralyzed limbs, caused primarily by post-SCI motor paralysis.

Quantitative evaluation of the muscle viscoelasticity and tone is important in preventing secondary disorders after SCI. The Modified Ashworth Scale (MAS) is generally used to measure muscle tone and spasticity,[9] but this score lacks adequate sensitivity to distinguish the contributions from the mechanical and neural components.[10] In a study of the neural profile after SCI, we reported that spinal reflex excitability in participants experiencing both complete and incomplete SCI are significantly higher than the excitability in healthy young participants, but the Hmax/Mmax did not change significantly in incomplete SCI participants.[11] In addition, the change in Hmax/Mmax was not associated with the chronicity of injury in SCI participants. Muscle viscoelasticity is a significant contributor to muscle tone, and it is therefore necessary to understand not only the neural but also the mechanical properties of the paralyzed region in SCI patients. To date, the relationship between the mechanical properties and the duration of injury has not been reported. This information could guide clinicians in determining the appropriate intervention for the patient's pathologic condition.

The objective of the present study is to determine the effect of injury duration on plantar-flexor elastic properties in individuals with chronic SCI and spasticity.

PATIENTS AND METHODS

Participants

Sixteen participants diagnosed with SCI (age, 33 ± 9 years; height, 172 ± 7 cm; weight, 62 ± 10 kg; injury localization, C6-T12; injury duration, 11–371 months) and spasticity (10 complete and 6 incomplete), five participants with complete SCI without spasticity (age, 30 ± 7 years; height, 174 ± 4 cm; weight, 67 ± 14 kg; injury localization, T9–L3; injury duration, 12–213 months) and 13 healthy control participants (age, 27 ± 5 years; height, 169 ± 10 cm; weight, 62 ± 10 kg; 10 male and 3 female) participated in this study. The population demographics

[1]Department of Life Sciences, Graduate School of Arts and Sciences, The University of Tokyo, Tokyo, Japan; [2]Department of Rehabilitation for the Movement Functions, Research Institute, National Rehabilitation Center for Persons with Disabilities, Saitama, Japan and [3]Division of Functional Control System, Graduate School of System engineering and Science, Shibaura Institute of Technology, Saitama, Japan
Correspondence: Dr N Kawashima, Department of Rehabilitation for the Movement Functions, Research Institute, National Rehabilitation Center for Persons with Disabilities, 4-1, Namiki, Tokorozawa, Saitama 359-855, Japan.
E-mail: kawashima-noritaka@rehab.go.jp
Received 23 April 2014; revised 29 October 2014; accepted 11 November 2014

Table 1 Population demographics

Subject	*Sex*	*Age (years)*	*Height (cm)*	*Weight (kg)*	*Lesion level*	*Injury type*	*With spasticity*	*MAS*	*Duration of injury (months)*	*Medication*
1	M	20	181	57	C6	Incomplete	Yes	2	11	Gabalon
2	M	30	170	71	T7	Incomplete	Yes	2	14	—
3	M	22	178	64	C7	Incomplete	Yes	2	18	ITB
4	M	45	171	64	T1	Incomplete	Yes	2	19	—
5	M	49	173	70	T3, 4, 5	Incomplete	Yes	1+	52	Dantrium, lendormin
6	M	25	170	54	T5	Incomplete	Yes	1+	63	—
7	M	23	175	61	T10	Complete	Yes	1+	18	—
8	M	27	178	55	T11, 12	Complete	Yes	2	30	—
9	F	27	172	50	T8, 9, 10	Complete	Yes	0	36	—
10	M	27	171	62	T10, 11	Complete	Yes	1	114	—
11	M	37	180	75	T12	Complete	Yes	1	115	Ternelin
12	M	35	173	62	T9, 10	Complete	Yes	1	144	—
13	M	33	174	77	T12	Complete	Yes	1+	144	—
14	M	39	174	77	T8	Complete	Yes	1+	155	—
15	F	40	163	55	T9	Complete	Yes	1+	300	—
16	F	48	153	40	T5	Complete	Yes	1	371	—
17	M	27	173	55	L3	Complete	No	—	12	—
18	M	30	175	58	Th12,L1,L2	Complete	No	—	15	—
19	M	21	178	60	Th9	Complete	No	—	23	—
20	M	33	175	87	Th11,12	Complete	No	—	198	—
21	M	41	168	75	Th10	Complete	No	—	213	—

Abbreviations: MAS, Modified Ashworth Scale, ITB, intrathecal baclofen therapy.
Healthy control subjects ($n=13$): age, 27 ± 6; height, 169 ± 10; weight, 62 ± 10.

Table 2 A: partial correlation coefficient between mechanical properties and injury duration (months), excluding muscle architecture and injury level. B: associated *P*-values

	Calf circumference (mm)	*MG (mm)*	*LG (mm)*	*Sol (mm)*	*Level of injury*
A					
Peak torque (Nm)	−0.70	−0.63	−0.80	−0.72	−0.79
Energy (Nm per deg)	−0.70	−0.33	−0.72	−0.58	−0.67
SI_{SOP} (Nm per deg)	−0.69	−0.57	−0.78	−0.69	−0.77
SI_{FOP} (Nm per deg)	−0.70	−0.63	−0.80	−0.72	−0.79
SI_{SK} (Nm per deg)	−0.45	−0.25	−0.62	−0.57	−0.65
$Angle_{SLACK}$ (Nm per deg)	0.58	0.42	0.71	0.63	0.72
B					
Peak torque (Nm)	0.017	0.039	0.003	0.019	0.004
Energy (Nm per deg)	0.017	0.319	0.012	0.077	0.024
SI_{SOP} (Nm per deg)	0.019	0.070	0.005	0.027	0.006
SI_{FOP} (Nm per deg)	0.016	0.038	0.003	0.018	0.004
SI_{SK} (Nm per deg)	0.163	0.461	0.042	0.087	0.032
$Angle_{SLACK}$ (Nm per deg)	0.061	0.201	0.014	0.052	0.013

Abbreviations: LG, lateral gastrocnemius; MG, medial gastrocnemius; Sol, soleus.

are summarized in Table 1. There was no statistical age difference among the three groups (SCI participants with spasticity, SCI participants without spasticity and healthy participants; F-value $=2.075$, $P=0.1422$). Each participant provided written informed consent for the experimental procedure, which was approved by the National Rehabilitation Center for Persons with Disabilities (NRCD).

Measurements

The participants were seated with their hip and knee joints angled at 90°. The ankle joint was fixed onto the foot plate of a custom dynamometer.[12] The calf circumference and muscle thickness of the plantar-flexors were measured at 30% of the calf length using a tape measure and ultrasonography (Prosound 2, Aloka, Tokyo, Japan) with a linear array probe (7.5 MHz). The calf circumference, medial gastrocnemius (Gas (MG)) and lateral Gas thicknesses of participants 5, 6 and 8, and four healthy control participants, as well as the soleus (Sol) thickness of participants 1, 5, 6 and 8, and five healthy control participants, were not obtained. We have stated that this lack of data might lead to type I error. The right ankle joint was rotated from 10° of plantar-flexion to 20° dorsiflexion at 5 deg s^{-1}. During the measurement, ankle joint angle and plantar-flexion torque were recorded at a 1 kHz sampling frequency using a 16-bit analog-to-digital converter (Powerlab, AD Instruments, Bella Vista, NSW, Australia). The muscle activity of the Gas, Sol and tibialis anterior were also measured using surface electromyograms with a bipolar electrode (DE-2.3, Delsys, Boston, MA, USA) spaced 1 cm apart. The electromyograms signal was amplified (The Bagnoli-8 EMG System, Delsys) with band-pass filtering between 20 Hz and 450 Hz. Some participants (#1, 2, 3, 4 and 5 in Table 2) had clonus. In those participants, therefore, we took care not to miss the emergence of symptoms by visually monitoring the joint motion and the surface electromyography displayed on an oscilloscope, and if clonus occurred, the experiment was temporarily stopped. The trial was repeated 6–10 times,